形状創成メカニズムを考慮した軸対称面研削の高精度化

Improvement of Form Accuracy in Axisymmetrical Grinding by Considering the Form Generation Mechanism

榎本　俊之*　島崎　裕*　谷　泰弘**　佐田　登志夫***
Toshiyuki ENOMOTO　Yutaka SHIMAZAKI　Yasuhiro TANI　Toshio SATA

要　旨

軸対称面を研削加工すると，目標形状に対し加工面が凹面に精度劣化してしまうという問題が生じる．そこで本研究では，加工実験，解析を通じて形状創成メカニズムを検討し，次にその解明されたメカニズムをもとに，高い形状精度の得られる加工法の提案を行った．具体的には，加工中，加工面の外周付近では砥石結合剤と工作物とが強く接触し，研削性（砥石切れ味）が劣化し，そのために形状が凹面に精度劣化することが判明した．そこで，加工面全面で砥石結合剤と工作物とが強く接触しないように，工作物中心より外周に向かって砥石をトラバースさせる加工を提案，実施した．その結果，120nm p-v以下の形状精度と20-40nm Ry の表面粗さを達成でき，高精度な研削加工を実現することができた．

ABSTRACT

Countermeasures are proposed to overcome the problem that, in grinding an axisymmetrical surface, the surface profile concavely deviates from the ideal profile. By experimental investigation of the form generation mechanism, it was found that the grindability deteriorated on the outward surface owing to direct contact between the wheel bond and the workpiece. Use of a hard bonded wheel improved form accuracy, and traversing the wheel outward from the workpiece center achieved both high form accuracy of less than 120 nm p-v with roughness ranging from 20 to 40 nm Ry.

* 研究開発本部　生産技術研究所
Manufacturing Technology R&D Center,
Research and Development Group
** 東京大学
The University of Tokyo
***豊田工業大学
Toyota Technological Institute

1. Introduction

Axisymmetrical, in particular, axisymmetrical aspherical devices such as lenses, mirrors, and molding dies, have been widely used in optical technology[1]. While generating the device profile, one often encounters problems such as the ground surface profile being concavely deviated from the ideal profile. To improve the form accuracy, compensation grinding—in which tool setting is corrected and tool trace data are modified—has been conventionally carried out[2]. However, since this method ignores elastic deformation[3] of the grinding wheel and the workpiece, high form accuracy cannot be obtained.

A commonly accepted explanation for the deterioration of form accuracy is as follows. The workpiece speed is higher on the outward surface. The generated grinding force increases as the workpiece speed increases[4] when the workpiece revolution and the wheel traversing speed are constant. This results in higher elastic deformation of the wheel and large residual removal on the outward surface. A machining method controlling the wheel traversing speed has been proposed so as to maintain a constant grinding force[5]. However, surface roughness deteriorates due to the higher feed rate changes at the workpiece center. Furthermore, high form accuracy of 0.1 μm p-v could not be obtained in this method, because the mechanism is not well understood.

To overcome this problem, it is essential to study the quantitative relationship between grinding force and generated form.

In this paper, we clarify the mechanism of generating form error by analyzing grindability in terms of grinding force, and also propose new methods to obtain high form accuracy based on the mechanism.

2. Experimental Procedure

The experimental setup has a T-shape configuration, as shown in Fig. 1. To achieve precise form generation of axisymmetrical aspherical surface, a contact between wheel and workpiece should be a point instead of an area. A wheel edge was used as a grinding point.

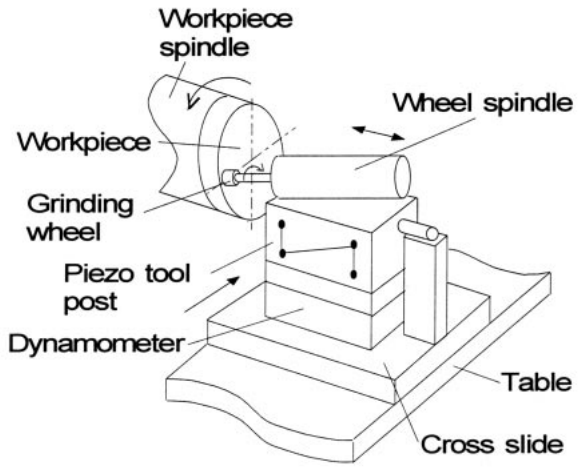

Fig.1 Experimental setup of precision grinding machine

The tool post has a piezo-electric actuator and a parallel link bearing system to position a tool with high resolution. This has a bandwidth of 55 Hz and 15nm positioning accuracy over the total range of 8μm using microprocessor closed loop control. The grinding machine is supported by four pneumatic isolators. The workpiece spindle with aerostatic bearings is driven by an AC motor via a belt coupling. The table is supported by hydrostatic oil guides and driven by a ball screw. The wheel spindle is driven by an air turbine. A workpiece is screwed into a magnetic jig, which is attached to the workpiece spindle by a permanent magnet.

Grinding forces were measured by a piezo-electric three-component dynamometer. The displacements of the tool post and the wheel spindle shaft were monitored with a capacitance displacement detector and an eddy current displacement detector, respectively. After grinding, the surface profile was in-situ measured with a stylus-type measuring instrument. From these data, an actual wheel depth of cut and a displacement of wheel were calculated.

Grinding conditions are shown in Table 1. Traversing direction, workpiece revolution speed, and wheel traversing speed were varied in 2 levels. A plane surface was used as a workpiece instead of a spherical or an aspherical surface to avoid form error caused by tool misalignment.

3. Analysis of form generation mechanism

3.1 Characteristics of inward traversing grinding

A typical example of a ground surface profile is shown in Fig. 2. In Exp. A through D, where the grinding wheel was traversed in the inward direction, the surface profiles obtained were concave, as shown in Fig. 2. It can be seen that residual removal increases drastically on the outward surface.

Figure 3 shows a typical example of a grinding force (data smoothed by moving average) compared with ground surface profiles. To measure the actual wheel depth of cut, a plastic ring having good machinability was pasted around the workpiece and was ground simultaneously. Changes in grinding force and surface profile can be understood by considering the explanation given in section1, that is, residual removal becomes large on the outward surface where workpiece speed is high and generated grinding force is large.

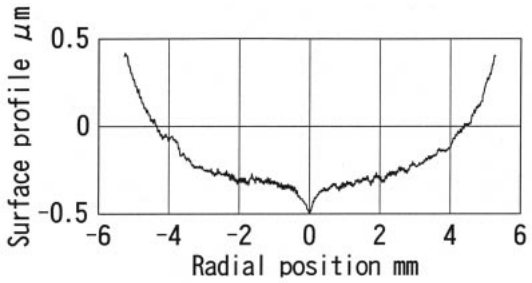

Fig.2 Profile of a ground surface (Exp.A)

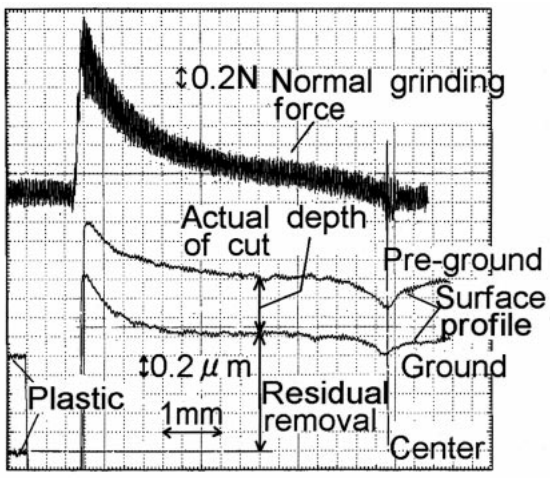

Fig.3 Grinding force and surface profiles (Exp.C)

Furthermore, the fact that the total removal of plastic was equal to the total depth of cut in several grinding experiments proves that wheel wear is negligible. In addition, the displacements of the tool post and the wheel spindle shaft are also negligible.

3.2 Mechanism based on conventional concept

Normal grinding force Fn(N) is generally given[4] by

$$Fn = P1 \times B \times t^{P2} \times (Vw/Vs)^{P3} \qquad (1)$$

where B(μm) : wheel contact width
t(μm) : actual wheel depth of cut
Vw(m/min) : workpiece speed
Vs(m/min) : grinding speed
$P1$,$P2$,$P3$: coefficients

The coefficients $P1$, $P2$, and $P3$ were computed by least squares fitting of the experimental results. In Exp. A through D, $P2$ was 0.9 and $P1$ ranged from 0.6 to 1.9, depending on the pass. On the other hand, $P3$ was not constant for all radial surface positions, as shown in Fig. 4.

This indicates that the grinding mechanism changed during a single pass. We recognize grindability as one of the key factors for characterizing the grinding condition. Grindability is often expressed in terms of grinding force ratio. The grinding force ratio (Fn/Ft) changes drastically on the outward surface (Ft is the tangential grinding force) as can be seen in Fig. 5.

Therefore, SEM observation of the wheel surface was carried out. An example photograph of scratch marks on the bonding surface is shown in Fig. 6. This indicates that bonding material came into contact with the workpiece. Direct contact between the bond and the workpiece has often been observed when a resinoid bonded wheel with fine grains was used[6].

Furthermore, an analysis of the measured grinding force confirmed that the dynamic component of the force is larger on the outward surface than on the inward one. This indicates that on the outward surface, that is, at the start of grinding, the changing rate of the grinding force is higher at the intermittent cutting condition. It is highly possible that direct contact between bonding

material and workpiece occurred. This direct contact causes the grinding force to increase, which in turn causes the direct contact to be stronger. In this way, grindability deteriorates drastically on the outward surface.

3.3 Mechanism of contact between wheel bond and workpiece

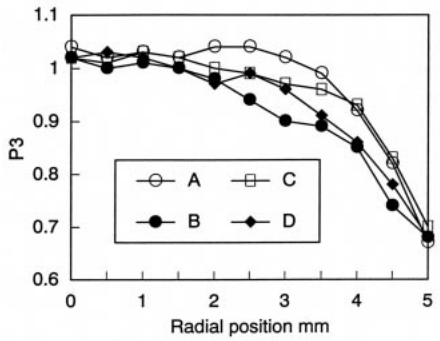

Fig.4 Change in coefficient P3 with radial position

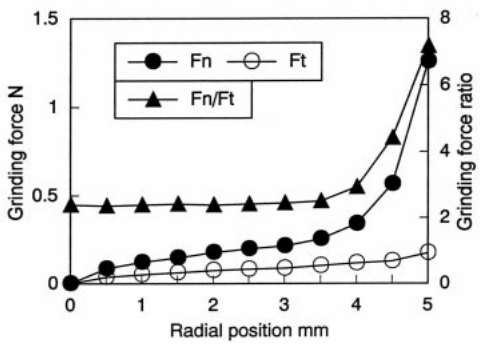

Fig.5 Change in grinding forces and force ratio (Exp.A)

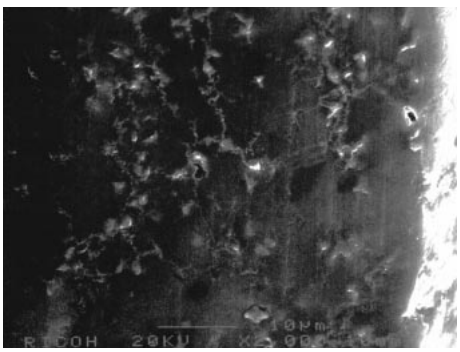

Fig.6 Grinding wheel surface after machining

Figure 7 shows a new grinding force model proposed, where contact between wheel bond and workpiece is taken into consideration. In this figure, measured grinding forces *Fn* and *Ft* are as follows:

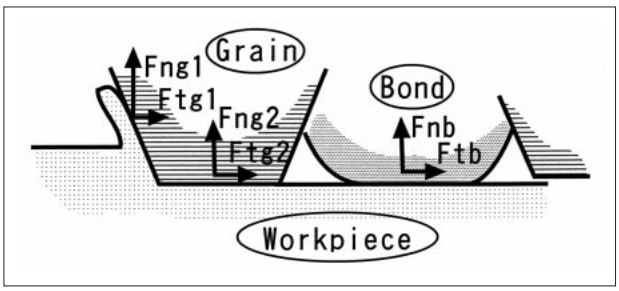

Fig.7 Grinding force model

$$Fn = Fng1 + Fng2 + \mathrm{Fnb}$$
$$= \lambda \times Ftg1 + Fng2 + Fnb \quad (2)$$
$$Ft = Ftg1 + Ftg2 + Ftb$$
$$= Ftg1 + \mu g \times Fng2 + \mu b \times Fnb \quad (3)$$

where *Fng1* and *Ftg1* : cutting force components
Fng2 and *Ftg2* : friction force components on grains
Fnb and *Ftb* : friction force components on bond
λ : cutting force ratio
μg and μb : friction coefficients of a grain and a bond against a workpiece, respectively

In Eq. (2) or (3), *Fng2* is proportional to the area of the grain flank[7]. Experimental results showed that the surface texture did not change on either outward or inward surface. This suggests that the area of the grain flank does not change. In addition, *Fng2* can be neglected, because *Fn* is almost zero at the workpiece center.
Therefore, Eqs. (2) and (3) become:

$$Fn = \lambda \times Ftg1 + Fnb$$
$$= P1 \times B \times t^{P2} \times (Vw/Vs)^{P3} + Fnb \quad (4)$$
$$Ft = Ftg1 + \mu b \times Fnb$$
$$= 1/\lambda \times P1 \times B \times t^{P2} \times (Vw/Vs)^{P3} + \mu b \times Fnb \quad (5)$$

From Eqs. (4) and (5), the following equation is obtained:

$$Ft = Ftg1 + \mu b \times (Fn - \lambda \times Ftg1)$$
$$= (1 - \mu b \times \lambda)/\lambda \times P1 \times B \times t^{P2} \times (Vw/Vs)^{P3} + \mu b \times Fn \quad (6)$$

The coefficients *P1, P2, P3, μb, λ* were calculated by least squares fitting. The results show that all parameters including *P3* are constant at all radial positions on the surface in Eq. (6) in contrast to Eq. (1). The *μb* is estimated to be in the order of 0.1 due to lubrication by the grinding fluid[8]. The obtained value, 0.13, is reasonable.

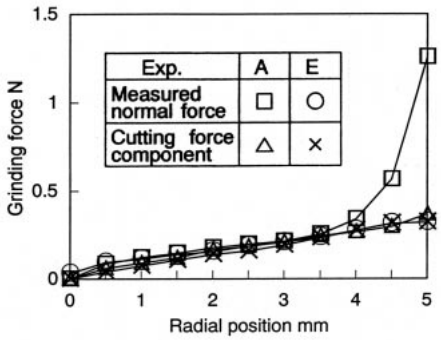

Fig.8 Change in mormal grinding force

Figure 8 shows the measured grinding force and the cutting force component calculated by Eq. (4). From this figure, we can consider the form generation mechanism in axisymmetrical grinding to be as follows. The cutting component is largest at the outward surface due to the high speed of workpiece. Under this condition, the bond easily makes contact with the workpiece. During inward traversing, the cutting component becomes smaller. As a result, the contact between the bond and the workpiece becomes smaller and so does the normal grinding force acting in the contact region. Thus, the residual removal increases on the outward surface and hence the surface profile becomes concave as shown in Fig. 2.

4. Methods for obtaining high form accuracy

One obvious way to prevent direct contact between the bond and the workpiece, and therefore to improve form accuracy, is to use a grinding wheel with a hard bonding material, such as a vitrified bond. Figure 9 shows the surface profiles of optical glasses ground by a resinoid bonded wheel and by a vitrified bonded wheel. Higher form accuracy is obtained by using a vitrified bonded wheel than by using a resinoid bonded wheel. However, surface roughness deteriorates. Typical roughness obtained by vitrified bonded wheel is ranging from 60 to 100nm Ry, while roughness ranging from 20 to 40 nm Ry can be obtained by resinoid bonded wheel. Therefore to obtain small roughness, a resinoid bonded wheel should be used in grinding.

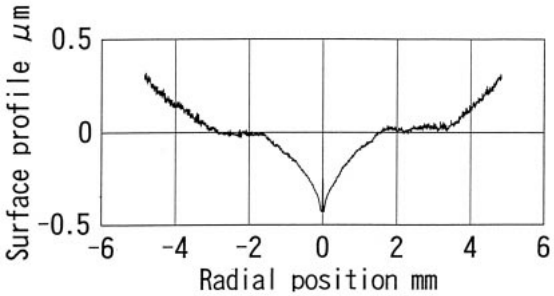

(a) Using SD3000N100B (resinoid bonded wheel)

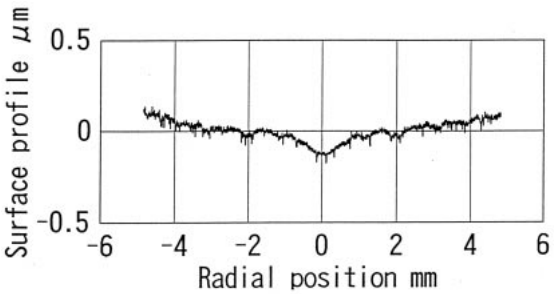

(b) Using SD3000N100v (vitrified bonded wheel)

Fig.9 Comparison of surface profiles obtained using different kinds of grinding wheels

However, decreased residual removal and resultant high form accuracy can be achieved with a resinoid bonded wheel by traversing in the outward direction from the workpiece center. The dynamic component of the grinding force is small at the workpiece center and the workpiece does not come strongly into contact with the bond. As the wheel is traversed outward, the cutting force component gradually increases, but the changing rate of the grinding force still stays low in the

intermittent cutting condition. As a result, the contact between the workpiece and the bond material becomes weaker during outward grinding pass.

Figure 10 shows the ground surface profile obtained by traversing in this manner, shown as, Exp. E in Table 1. The plane form accuracy obtained is 74 nm p-v. In a total of five grinding tests carried out under condition E, the form accuracies were less than 120 nm p-v and the surface roughnesses were almost the same as those of the inward traversing grinding. The measured grinding force and the cutting force component calculated by Eq. (4) are shown in Fig. 8. Compared with the experimental results for Exp. A, the force between the bond and the workpiece is small and the total grinding force does not increase on the outward surface. Furthermore, these results confirmed that the grinding force ratio, as a factor of the grindability, was almost constant in Exp. E.

Thus, traversing a wheel outward from the workpiece center allows grindability to be almost constant, and high form accuracy can be obtained.

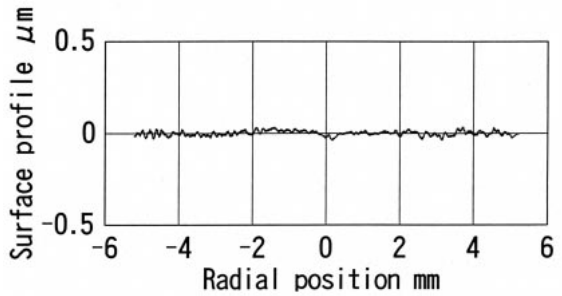

Fig.10 Profile of a ground surface (Exp.E)

Table 1 Grinding conditions

Grinding wheel	SD3000N100B				
Wheel contact width	110 μm				
Depth of cut	about 1 μm				
Grinding speed	570 m/min				
Workpiece	Tungsten carbide : φ 11mm				
Grinding fluid	Soluble type				
Exp. symbol	A	B	C	D	E
Traversing direction	outer → inner				inner →outer
Workpiece revolution rpm	200	350	200	350	200
Traversing speed mm/min	5.8	5.8	10.1	10.1	5.8

5. Conclusions

In grinding an axisymmetrical surface, the surface profile is concavely deviated from the ideal profile. By investigating the form generation mechanism, we can conclude that:

(1) In traversing the wheel inward toward the workpiece center, the bonding material of the wheel comes strongly into contact with the workpiece, so the grinding force is very strong on the outward surface. Therefore, residual removal increases on the outward surface and the surface profile deteriorates.

(2) Using a wheel having a hard bond, such as a vitrified bonded wheel, improves form accuracy by reducing the direct contact between the bond and the workpiece, but deteriorates the surface roughness.

(3) By traversing the wheel outward from the workpiece center, the bond does not come strongly into contact with the workpiece, and both high form accuracy of less than 120 nm p-v with roughness ranging from 20 to 40 nm Ry can be obtained.

References

1) K. Ueda et al. : Machining High-Precision Mirrors Using Newly Developed CNC Machine, Annals of the CIRP, 40, 1 (1991) pp.555-558.

2) T. Nishiguchi et al. : Improvement of Productivity in Aspherical Precision Machining with In-situ Metrology, Annals of the CIRP, 40, 1 (1991) pp.367-370.

3) D.P. Saini and J.G. Wager : Local Contact Deflections and Forces in Grinding, Annals of the CIRP, 34, 1 (1985) pp.281-285.

4) H.K. Töshoff et al. : Modelling and Simulation of Grinding Processes, Annals of the CIRP, 41, 2 (1992) pp.677-688.

5) H. Suzuki et al. : Study on Aspherical Grinding, Proceedings of Spring Conf. of JSPE, (1994) pp.799-800 (in Japanese).

6) L. Zhou, T. Kuriyagawa and K. Syoji : Truing, Dressing and Grinding Characteristics for Very Fine Grit Diamond Wheels, Journal of JSGE, 36, 4 (1991) pp.239-244 (in Japanese).

7) S. Hanasaki, M. Touge and Y. Hasegawa : Study on Electrolytic Grinding Mechanism by Using a Single Diamond Tool with Wear Flat Area, Journal of JSPE, 56, 1 (1990) pp.115-120 (in Japanese).

8) K. Sato : Studies on Plunge-Cut Grinding(2), Journal of JSPE, 22, 12 (1956) pp.503-507 (in Japanese).